

Searches for Rare Leptonic and Semileptonic Charm Decays at *BABAR*

Paul D. Jackson

*The Ohio State University,
Department of Physics and Astronomy,
191 West Woodruff Avenue,
Columbus, Ohio, 43210,
USA.
jack@slac.stanford.edu*

Received 20/August/2006

Recent results from leptonic and semi-leptonic charm decays at the *BABAR* B -factory are presented. The measurement of f_{D_s} from the $D_s^+ \rightarrow \mu^+ \nu$ channel is presented. Form-factor studies from the $D^0 \rightarrow K^+ e^- \bar{\nu}_e$ channel are described along with a search for flavor-changing neutral-current $X_c^+ \rightarrow h^+ \ell^+ \ell'^-$ decays.

Keywords: charm; leptonic; form-factor.

PACS numbers: 11.25.Hf, 123.1K

1. Introduction

B -factories have been successfully operating for more than 6 years, providing an unprecedented data sample of $e^+ e^-$ collisions producing hadrons. The *BABAR* experiment has collected almost 400 fb^{-1} at the $\Upsilon(4S)$ center-of-mass (CM) energy. At this energy, the cross-section for charm production is $\sigma(c\bar{c}) \simeq 1.3 \text{ nb}$. Indeed the B -factories can also be considered charm factories.

The *BABAR* detector operates at the PEP-II B -factory and is optimized for asymmetric $e^+ e^-$ collisions. The tracking system is composed of a 5-layer silicon vertex tracker and a 40-layer drift chamber along with a Cherenkov detector for charged particle identification and CsI calorimeter (EMC), they are all immersed in a 1.5-T solenoidal field, the return yoke of which is instrumented with resistive plate chambers (IFR) for muon and neutral hadron identification. A detailed description of the detector is given elsewhere ¹.

2. Precise measurement of the pseudoscalar decay constant f_{D_s} using charm-tagged events.

The measurement of leptonic weak decays of charmed pseudoscalar mesons can provide a determination of the overlap between the wavefunction of heavy and light

quarks within the meson, represented by the form factor f_M for each meson M . The partial width for a D_s^+ meson to decay weakly to a lepton ℓ is given by:

$$\Gamma(D_s^+) = \frac{G_F^2 |V_{cs}|^2}{8\pi} f_{D_s}^2 m_\ell^2 m_{D_d} \left(1 - \frac{m_\ell^2}{m_{D_s}^2}\right)^2, \quad (1)$$

where m_ℓ and m_{D_s} are the lepton and D_s masses, G_F is the Fermi constant and $|V_{cs}|$ is the CKM parameter for the annihilation of the quarks in the D_s . Predictions from lattice QCD have yielded $f_{D_s} = (249 \pm 17)$ MeV and $f_{D_s}/f_D = 1.24 \pm 0.07$ ². *BABAR* presented at this conference a preliminary result of the measurement of the ratio $\Gamma(D_s^+ \rightarrow \mu^+\nu)/\Gamma(D_s^+ \rightarrow \phi\pi^+)$ and of the decay constant f_{D_s} using a sample of 230 fb^{-1} of data. The $D_s^+ \rightarrow \mu^+\nu$ events are reconstructed from the decay chain $D_s^{*+} \rightarrow \gamma D_s^+$, $D_s^+ \rightarrow \mu^+\nu$, where the D_s^{*+} are produced in the hard fragmentation of continuum $c\bar{c}$ events. In the D_s^{*+} decay an energetic photon, a high-momentum D_s^+ and a daughter muon and neutrino are produced, all lying mostly in the same hemisphere of the event. The recoil system of a signal candidate is a fully reconstructed D^0 , D^+ , D_s^+ or D^{*+} (referred to as the tag system), wherein the tag flavor, and the charge of the signal muon, are uniquely determined. A minimum tag momentum close to the kinematic limit for charm mesons produced from B decays is required in order to reduce B backgrounds. The D_s^{*+} signal is reconstructed from a muon and a photon candidate in the recoil of the tag. Muons are identified using the IFR and must have a momentum of greater than $1.2 \text{ GeV}/c$ in the CM frame and a charge consistent with the tag flavor. Energy deposits in the EMC with no associated charged track are identified as photon candidates whose CM energy must be greater than 0.115 GeV . The total missing energy and momentum (E_{miss}^* , p_{miss}^*) in the CM is computed using the four-momenta of the incoming e^+e^- and the measured four momenta of all tracks and photons in the event. To take into account that the neutrino in the signal decay leads to a large missing energy in the event, signal candidates are selected requesting $E_{\text{miss}}^2 > 0.38 \text{ GeV}$. The CM four-momentum of the D_s^+ candidate is obtained by combining the CM four-momentum of the muon and the neutrino. The D_s^+ candidate is then combined with a photon candidate to form a D_s^{*+} . Signal events are required to have $|\vec{p}_{D_s^{*+}}| > 3.55 \text{ GeV}/c$. The signature of the $D_s^{*+} \rightarrow \gamma D_s^+$ decay is a narrow peak in the distribution of the mass difference $\Delta M = M(\mu\nu\gamma) - M(\mu\nu)$ at $143.5 \text{ MeV}/c^2$.

There are several distinct sources of background that have been accounted for in the analysis. The first type of backgrounds are from $e^+e^- \rightarrow f\bar{f}$ events (where $f = u, d, s, b$ or τ) which do not contain a real charm tag or $e^+e^- \rightarrow c\bar{c}$ events where the tag is incorrectly reconstructed. The contribution of these events is estimated from real data using the tag sidebands. The second type of background events are correctly tagged $c\bar{c}$ events with the selected muon coming from a semileptonic charm decay or $\tau^+ \rightarrow \mu^+\nu_\mu\bar{\nu}_\tau$. The size and shape of this contribution is estimated by repeating the analysis substituting a well-identified electron for the muon. These events are weighted with the ratio of muon to electron efficiency. Remaining back-

grounds are estimated using Monte Carlo simulations.

Events selected in the analysis are grouped in four sets, according to whether the tag is in the signal or sideband region and on whether the selected lepton is a muon or an electron. The ΔM distribution for events in the tag sidebands are subtracted from the signal distribution, as are the electron events from the muon ones. The resulting distributions, presented in Figure 1, are fit with the function $(N_{\text{sig}} f_{\text{sig}} + N_{\text{bg}} f_{\text{bg}}) \cdot \Delta M$, where f_{sig} and f_{bg} describe the simulated signal and background ΔM distributions. All parameters in the fit are fixed except the yields of signal, N_{sig} , and background, N_{bg} . The result of the fit yields $N_{\text{sig}} = 489 \pm 55(\text{stat.})$ events.

Since the $D_s^{(*)+}$ production rate in $c\bar{c}$ is unknown, the partial width ratio $\Gamma(D_s^+ \rightarrow \mu^+\nu)/\Gamma(D_s^+ \rightarrow \phi\pi^+)$ is computed by reconstructing the decay chain $D_s^{*+} \rightarrow \gamma D_s^+$, $D_s^+ \rightarrow \phi\pi^+$ and the $D_s^+ \rightarrow \mu^+\nu$ branching fraction is computed using the measured $D_s^+ \rightarrow \phi\pi^+$ branching fraction.

Candidate ϕ mesons are reconstructed from two kaons of opposite sign and then combined with a charged pion to form a D_s^+ candidate. Photon candidates are then combined with the reconstructed D_s^+ to form D_s^{*+} candidates. The same requirements are imposed on the photon CM energy and D_s^+ momentum as in the $D_s^+ \rightarrow \mu^+\nu$ selection. Data are then grouped according to whether the tag lies in the signal or sideband region. The tag sideband ΔM region is subtracted from the signal region as mentioned above and the same fit performed yielding $N_{\phi\pi} = 2065 \pm 95(\text{stat.})$ events, see Fig. 1. The presence of two charged kaons in the $D_s^+ \rightarrow \phi\pi^+$ events leads to an increase in the number of random tag combinations with respect to $D_s^+ \rightarrow \mu^+\nu$ events. The correction for this effect is determined from MC and is found to be 1.4%. The effect of a difference between data and MC in the D_s^{*+} spectrum is measured by selecting $D_s^{*+} \rightarrow \gamma D_s^+$, $D_s^+ \rightarrow \phi\pi^+$ events in data and removing the requirement on $|\vec{p}_{D_s^{*+}}|$. A harder momentum spectrum is observed

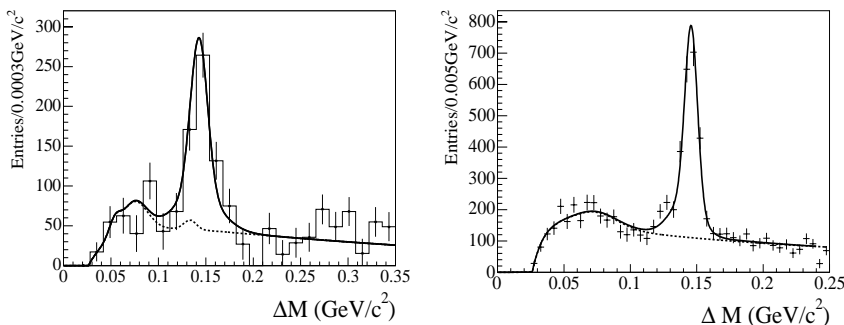


Fig. 1. (left) ΔM distribution for $D_s^+ \rightarrow \mu^+\nu$ events after the tag sidebands and the electron sample are subtracted. The solid line is the fitted signal+background distribution while the dotted line is the background only distribution. (right) ΔM distribution for $D_s^+ \rightarrow \phi\pi^+$ events after the tag sidebands are subtracted. The solid line is the fitted signal+background distribution while the dotted line is the background only distribution.

in data when efficiency corrected D_s^{*+} events are compared with those selected from MC. Therefore, the detection efficiencies for signal $D_s^{*+} \rightarrow \gamma D_s^+$, $D_s^+ \rightarrow \phi\pi^+$ events are re-evaluated after weighting the simulated events to match the D_s^+ momentum spectrum in data. Upon applying these efficiency corrections, the partial width ratio is determined to be $\Gamma(D_s^+ \rightarrow \mu^+\nu)/\Gamma(D_s^+ \rightarrow \phi\pi^+) = 0.136 \pm 0.017(\text{stat.})$ with $\mathcal{B}(\phi \rightarrow K^+K^-) = 49.1\%$ ³.

The total systematic uncertainty in $\Gamma(D_s^+ \rightarrow \mu^+\nu)/\Gamma(D_s^+ \rightarrow \phi\pi^+)$ is 4.6% and is dominated by the systematic error in the signal efficiency and the uncertainty arising from a possible inadequate parameterization of the signal and background shapes.

Using the *BABAR* measurement $\mathcal{B}(D_s^+ \rightarrow \phi\pi^+) = 4.81 \pm 0.64\%$ ⁴, the branching fraction $\mathcal{B}(D_s^+ \rightarrow \mu^+\nu) = (6.5 \pm 0.8 \pm 0.3 \pm 0.9) \times 10^{-3}$ and the decay constant $f_{D_s} = (279 \pm 17 \pm 6 \pm 19)$ MeV are obtained. The third error in the measurement is due to the uncertainty in the $D_s^+ \rightarrow \phi\pi^+$ branching fraction. The ratio of f_{D_s} to f_D from the CLEO-c measurement is $f_{D_s}/f_D = 1.25 \pm 0.14$ and is consistent with the lattice QCD prediction.

3. Form factor measurement from semileptonic $D^0 \rightarrow K^+e^-\bar{\nu}_e$ decay.

At this conference we presented a measurement of the q^2 variation of the hadronic form factor in the decay $D^0 \rightarrow K^+e^-\bar{\nu}_e$. A detailed description of this analysis can be found in the literature⁵. Neglecting the electron mass there is contribution from a single form factor. Furthermore, as this decay is induced by a vector current generated by the c and \bar{s} quarks the q^2 variation of the form factor $f_+(q^2)$ is governed by the D_s^{*+} pole. The following expressions have been proposed⁶:

$$|f_+(q^2)| = \frac{f_+(0)}{1 - \frac{q^2}{m_{\text{pole}}^2}}, \quad (2)$$

$$|f_+(q^2)| = \frac{f_+(0)}{\left(1 - \frac{q^2}{m_{D_s^*}^2}\right)\left(1 - \frac{\alpha_{\text{pole}} q^2}{m_{D_s^*}^2}\right)}. \quad (3)$$

Equation 2 is the “pole mass” and Equation 3 is the “modified pole mass”. Each distribution depends on a single parameter: m_{pole} and α_{pole} respectively. In Equation 3, $m_{D_s^*}$ is the physical D_s^* mass. In lattice QCD calculations a “lattice mass” is commonly used for $m_{D_s^*}$ but the computed value for α_{pole} is expected to be directly comparable to the value extracted from the fit to data using equation 3. A recent lattice QCD computation gives $\alpha_{\text{pole}}^{\text{lattice}} = 0.50 \pm 0.04$ ⁷.

The analysis presented herein uses the *BABAR* data taken between February 2000 and June 2002 corresponding to an integrated luminosity of 75 fb^{-1} . The analysis is based on the reconstruction of D^{*+} mesons produced in continuum $c\bar{c}$ events in which $D^{*+} \rightarrow D^0\pi^+$ and the D^0 decays semileptonically.

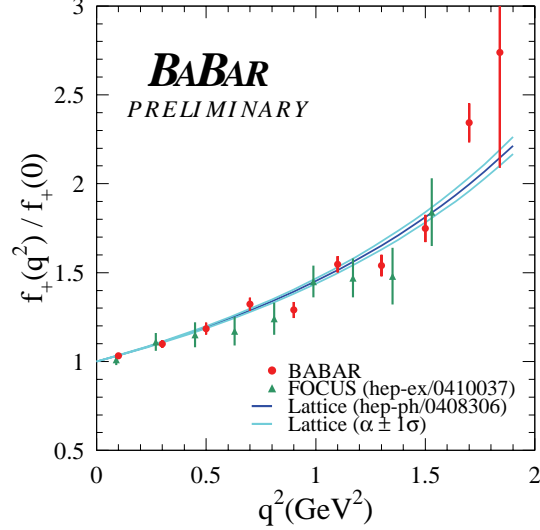


Fig. 2. Comparison between the measured variation of $\langle |f_+(q^2)| \rangle$ obtained in this analysis and with the FOCUS experiment. The band corresponds to expectations from lattice QCD calculations.

Electron candidates are selected with momentum greater than 0.5 GeV/c and the direction of the event thrust axis is taken as $|\cos(\theta_{\text{thrust}})| < 0.6$. R2⁸, the ratio between the zeroth and second Fox–Wolfram moments, and the total charged and neutral multiplicity are used to reduce the background from B events by exploiting their spherical nature. Charged and neutral objects are boosted into the CM system and the event thrust axis is determined. A plane perpendicular to the thrust axis, and containing the beam interaction point, is used to define two event hemispheres. Each hemisphere is considered in turn for having an electron(\pm), a kaon(\mp) and a pion(\pm) reconstructed and with the correct relative charges. Constrained fits to the D^0 and D^{*+} masses are imposed to evaluate the neutrino (ν_e) momentum. After performing the fit to the D^0 mass events with a χ^2 probability greater than 10^{-3} are retained. Herein, we evaluate $q^2 = (p_D - p_K)^2 (= (p_e + p_{\nu_e})^2)$ where p_D and p_K are the four momenta of the D and K mesons respectively. To obtain the unfolded q^2 distribution for signal events, corrected for resolution and acceptance effects, the Singular Value Decomposition (SVD)⁹ of the resolution matrix has been used in conjunction with a regularization which minimizes the curvature of the correction distribution. Results from this analysis on the q^2 variation of the hadronic form factor have been compared in Figure 2 with FOCUS¹⁰ measurements and with the lattice QCD⁷ evaluation.

Fitting the pole mass and the modified pole mass to the measurements we obtain values for the parameter that governs their q^2 dependence:

$$m_{\text{pole}} = (1.854 \pm 0.016 \pm 0.020) \text{ GeV}/c^2; \quad \alpha_{\text{pole}} = 0.43 \pm 0.03 \pm 0.04 \quad (4)$$

where the first error is statistical and the second error is systematic. In the modified pole model this can be interpreted as evidence for the contribution from other vector states of invariant mass higher than the D_s^{*+} mass. The value obtained for α_{pole} agrees with the one obtained from lattice QCD.

4. Search for Flavor-Changing Neutral-Current Charm Decays

A search for the decay modes $D_{(s)}^+ \rightarrow \pi^+ \ell^+ \ell'^-$, $D_{(s)}^+ \rightarrow K^+ \ell^+ \ell'^-$ and $\Lambda_c \rightarrow p \ell^+ \ell'^-$ has been performed using 288 fb^{-1} of $e^+ e^-$ data. A detailed description of this analysis can be found in the literature¹¹. In the Standard Model flavor-changing neutral-currents (FCNC) cannot occur at the tree level and therefore provide an excellent window in which to search for new physics. FCNC processes have been studied extensively in B and K systems but in the charm sector have received less attention. In the analysis presented here we combine an initial pion, kaon or proton with two tracks identified as leptons. We then study the invariant mass distribution of these combinations for consistency with a D^+ , D_s^+ or Λ_c candidate. A suite of mode dependent angular and kinematic criteria are imposed in order to optimize the search for each of the 20 possible modes. Criteria include ensuring that the dilepton system is not consistent with being produced by a ϕ meson. Searches for $D_{(s)}^+$ decay modes are normalized to the rate for $D_{(s)}^+ \rightarrow \pi^+ \phi$ and Λ_c decay mode searches are normalized to the $\Lambda_c \rightarrow p K^- \pi^+$ rate. Results for all modes are summarized in Table 1. No signals are observed and we obtain upper limits on the branching ratios $\frac{\Gamma(D_{(s)}^+ \rightarrow \pi^+ \ell^+ \ell'^-)}{\Gamma(D_{(s)}^+ \rightarrow \pi^+ \phi)}$, $\frac{\Gamma(D_{(s)}^+ \rightarrow K^+ \ell^+ \ell'^-)}{\Gamma(D_{(s)}^+ \rightarrow \pi^+ \phi)}$ and $\frac{\Gamma(\Lambda_c \rightarrow p \ell^+ \ell'^-)}{\Gamma(\Lambda_c \rightarrow p K^- \pi^+)}$ between 10^{-4} and 40×10^{-4} at 90% CL. This corresponds to limits on the branching fractions between 4×10^{-6} and 4×10^{-5} . These limits are calculated under the assumption of three-body phase-space decays; the efficiency varies by up to 25% as a function of dilepton invariant mass. For 17 out the 20 decay modes, the limits are an improvement over the existing measurements.

References

1. The BABAR Collaboration, B. Aubert *et al.*, Nucl. Instrum. Meth. **A479**, 1–116 (2002).
2. C. Aubin *et al.*, Phys. Rev. Lett. **95**, 122002 (2005).
3. Particle Data Group, S. Eidelman *et al.*, Phys. Lett. B **592**, 1 (2004).
4. The BABAR Collaboration, B. Aubert *et al.*, Phys. Rev. D **71**, 091104 (2005).
5. [arXiv:hep-ex/0607077].
6. J. G. Koerner and G. A. Schuler, Z.Phys. **C38** (1988) 511; Erratum-ibid, **C41** (1989) 690. M. Bauer and M. Wirbel, Z. Phys. **C42** (1989) 671.
D. Becirevic and A. B. Kaidalov, Phys. Lett. B. **478** (2000) 417.
7. C. Aubin *et al.*, Phys. Rev. Lett. **94**, 011601 (2005).
8. G. C. Fox and S. Wolfram, Phys. Rev. Lett. **41**, 1581 (1978).
9. A. Hoecker and V. Kartvelishvili, Nucl. Inst. Meth. A **372**, 469 (1996).
10. J. M. Link *et al.*, FOCUS collaboration, Phys. Lett. B **607**, 233 (2005).
11. [arXiv:hep-ex/0607051].

Table 1. Yields from fits to the candidates in the $20 X_c^+ \rightarrow h^+ \ell^+ \ell^-$ decay modes. The first error is statistical and the second the systematic error on the yield. The third column shows the estimated signal efficiency. The fourth column shows the 90% CL upper limits on the branching ratios of the signal mode to the normalization mode. The last column shows the limits on the branching fraction for the signal modes at 90% CL. The upper limits include all systematic uncertainties.

Decay mode	Yield (events)	Efficiency	BR (10^{-4}) (90% CL)	BF (10^{-6}) (90% CL)
$D^+ \rightarrow \pi^+ e^+ e^-$	$24.0^{+25.0+3.4}_{-24.1-5.1}$	3.93%	< 17.7	< 11.2
$D^+ \rightarrow \pi^+ \mu^+ \mu^-$	$1.5^{+20.1+3.4}_{-19.3-2.6}$	1.09%	< 38.7	< 24.4
$D^+ \rightarrow \pi^+ e^+ \mu^-$	$4.1^{+17.8+3.1}_{-16.3-2.1}$	2.27%	< 17.1	< 10.8
$D^+ \rightarrow \pi^+ \mu^+ e^-$	$-12.1^{+15.5+3.2}_{-14.8-0.0}$	2.29%	< 9.3	< 5.9
$D_s^+ \rightarrow \pi^+ e^+ e^-$	$-1.7^{+5.3+0.2}_{-4.6-2.0}$	1.14%	< 2.1	< 7.6
$D_s^+ \rightarrow \pi^+ \mu^+ \mu^-$	$-9.4^{+5.0+0.2}_{-4.4-1.4}$	0.31%	< 5.1	< 18.5
$D_s^+ \rightarrow \pi^+ e^+ \mu^-$	$4.8^{+4.7+0.8}_{-3.9-0.3}$	0.66%	< 6.2	< 22.3
$D_s^+ \rightarrow \pi^+ \mu^+ e^-$	$0.5^{+4.0+1.0}_{-3.3-0.1}$	0.65%	< 3.8	< 13.9
$D^+ \rightarrow K^+ e^+ e^-$	$5.9^{+8.9+3.8}_{-7.8-0.3}$	3.21%	< 8.2	< 5.2
$D^+ \rightarrow K^+ \mu^+ \mu^-$	$2.9^{+8.0+0.2}_{-7.0-3.7}$	0.75%	< 22.2	< 14.0
$D^+ \rightarrow K^+ e^+ \mu^-$	$-3.4^{+6.5+1.0}_{-5.6-0.1}$	1.64%	< 5.7	< 3.6
$D^+ \rightarrow K^+ \mu^+ e^-$	$-4.4^{+7.1+1.4}_{-6.1-3.0}$	1.64%	< 5.9	< 3.7
$D_s^+ \rightarrow K^+ e^+ e^-$	$-3.8^{+6.2+1.5}_{-5.3-1.3}$	2.81%	< 1.8	< 6.6
$D_s^+ \rightarrow K^+ \mu^+ \mu^-$	$5.0^{+6.5+0.1}_{-6.1-0.3}$	0.68%	< 7.1	< 25.4
$D_s^+ \rightarrow K^+ e^+ \mu^-$	$-3.7^{+5.1+1.4}_{-4.4-1.4}$	1.40%	< 1.5	< 5.6
$D_s^+ \rightarrow K^+ \mu^+ e^-$	$-6.5^{+4.9+0.2}_{-4.3-1.1}$	1.40%	< 1.0	< 3.6
$\Lambda_c \rightarrow p e^+ e^-$	$0.9^{+4.1+0.4}_{-3.4-0.1}$	4.11%	< 0.7	< 3.6
$\Lambda_c \rightarrow p \mu^+ \mu^-$	$6.9^{+4.7+0.3}_{-3.7-0.6}$	0.67%	< 8.1	< 40.4
$\Lambda_c \rightarrow p e^+ \mu^-$	$0.2^{+2.9+0.5}_{-2.0-0.5}$	1.19%	< 1.8	< 8.9
$\Lambda_c \rightarrow p \mu^+ e^-$	$-0.2^{+2.5+0.5}_{-1.7-0.9}$	1.18%	< 1.5	< 7.5